

# CHEMISTRY

## A European Journal

A Journal of



### Accepted Article

**Title:** Molecular Packing and Solid-state Photophysical Properties of 1,3,6,8-Tetraalkylpyrenes

**Authors:** Takanori Iwasaki, Shin Murakami, Youhei Takeda, Gaku Fukuhara, Norimitsu Tohnai, Yumi Yakiyama, Hidehiro Sakurai, and Nobuaki Kambe

This manuscript has been accepted after peer review and appears as an Accepted Article online prior to editing, proofing, and formal publication of the final Version of Record (VoR). This work is currently citable by using the Digital Object Identifier (DOI) given below. The VoR will be published online in Early View as soon as possible and may be different to this Accepted Article as a result of editing. Readers should obtain the VoR from the journal website shown below when it is published to ensure accuracy of information. The authors are responsible for the content of this Accepted Article.

**To be cited as:** *Chem. Eur. J.* 10.1002/chem.201903224

**Link to VoR:** <http://dx.doi.org/10.1002/chem.201903224>

Supported by  
**ACES**

WILEY-VCH

## FULL PAPER

## Molecular Packing and Solid-state Photophysical Properties of 1,3,6,8-Tetraalkylpyrenes

Takanori Iwasaki,<sup>\*,[a][b]</sup> Shin Murakami,<sup>[a]</sup> Youhei Takeda,<sup>[a]</sup> Gaku Fukuhara,<sup>[c]</sup> Norimitsu Tohnai,<sup>[d]</sup> Yumi Yakiyama,<sup>[a]</sup> Hidehiro Sakurai,<sup>[a]</sup> Nobuaki Kambe<sup>\*,[a]</sup>

**Abstract:** The relationship between the photophysical properties and molecular orientation of 1,3,6,8-tetraalkylpyrenes in the solid state is described herein. The introduction of alkyl groups with different chain structures (in terms of length and branching) did not affect the photophysical properties in solution, but significantly shifted the emission wavelengths and fluorescence quantum yields in the solid state for some samples. Pyrenes bearing Et, *iso*Bu, or *neo*Pen groups at the 1-, 3-, 6-, and 8-positions showed similar emission profiles in both the solution and solid states. In contrast, pyrenes bearing other alkyl groups exhibited an excimer emission in the solid state, similar to that of the parent pyrene. On studying the photophysical properties in the solid state with respect to the obtained crystal structures, the observed solid-state photophysical properties were found to depend on the relative position of the pyrene chromophores. The solid-state photophysical properties can be controlled by the alkyl groups, which provide changing crystal packing. Among the pyrenes tested, 1,3,6,8-tetraethylpyrene showed the highest fluorescence quantum yield of 0.88 in the solid state.

characterized.<sup>[1]</sup> To modulate the photophysical properties of pyrene, various pyrene derivatives have been developed by incorporating (hetero)aryl,<sup>[2]</sup> alkenyl,<sup>[3]</sup> alkynyl,<sup>[4]</sup> and heteroatom groups<sup>[5]</sup> into the pyrene core. Regulating the photophysical properties such as fluorescence wavelength, quantum yields, and lifetimes of pyrenes in solution can be achieved by introducing the aforementioned substituents. However, the solid-state photophysical behaviors are responsible for the intrinsic single-molecular properties and self-assembled molecular orientations originating from their unique stacking characteristics (Figure 1). To date, various approaches for controlling the photophysical properties of pyrene derivatives in the solid state, as well as in films and micelles, have been reported.<sup>[6]</sup> However, rational and reliable strategies to predict their photophysical properties in the solid state have not yet been established. Therefore, the systematic examination of the effects of molecular orientation of substituted pyrenes on their solid-state photophysical properties remains as a significant knowledge gap.

## Introduction

Pyrene is a polycyclic aromatic hydrocarbon with high prospects to be used in the fields of physical chemistry and material sciences, and its photophysical properties have been well-

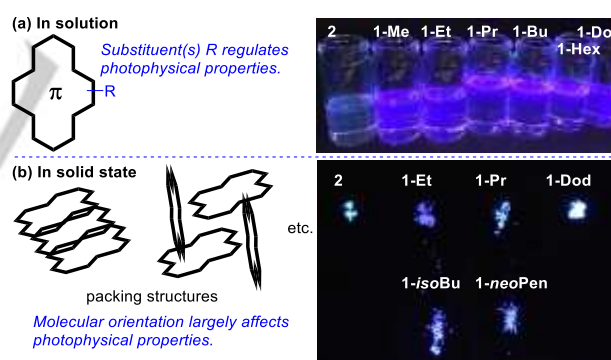


**Figure 1.** Photophysical properties of 1,3,6,8-tetraalkylpyrenes **1** and pyrene **2** in the solution and solid.

In general, alkyl substituents in  $\pi$ -systems do not significantly change the optical properties of the resulting derivative but greatly affect the molecular orientation through steric hindrance in the solid state. Therefore, introduction of alkyl groups into  $\pi$ -conjugated molecules can provide useful information regarding the relationship between molecular orientations and solid-state photophysical properties.<sup>[7-9]</sup> Kitamura *et al.* reported that, in the solid state, the UV/vis spectra of 1,4,7,10-tetraalkyltetracenes strongly depended on the length of the alkyl substituents.<sup>[10]</sup> Similarly, UV/vis and fluorescence spectral changes by varying the alkyl chain lengths have been reported for a number of  $\pi$ -conjugated systems.<sup>[11]</sup> Konishi *et al.* prepared pyrene derivatives

[a] Prof. Dr. T. Iwasaki, S. Murakami, Prof. Dr. Y. Takeda, Prof. Dr. Y. Yakiyama, Prof. Dr. H. Sakurai, Prof. Dr. N. Kambe  
Department of Applied Chemistry, Graduate School of Engineering  
Osaka University  
Suita, Osaka 565-0871 (Japan)  
E-mail: kambe@chem.eng.osaka-u.ac.jp

[b] Prof. Dr. T. Iwasaki  
Department of Chemistry and Biotechnology, Graduate School of Engineering  
The University of Tokyo  
7-3-1 Hongo, Bunkyo-ku, Tokyo 113-8656 (Japan)  
E-mail: iwasaki@chembio.t.u-tokyo.ac.jp

[c] Prof. Dr. G. Fukuhara  
Department of Chemistry, Tokyo Institute of Technology  
2-12-1 Ookayama, Meguro-ku, Tokyo 152-8551 (Japan)  
and  
JST, PRESTO, 4-1-8 Honcho, Kawaguchi, Saitama, 332-0012 (Japan)

[d] Prof. Dr. N. Tohnai  
Department of Material and Life Science, Graduate School of Engineering  
Osaka University  
Suita, Osaka 565-0871 (Japan)

Supporting information for this article is given via a link at the end of the document.

## FULL PAPER

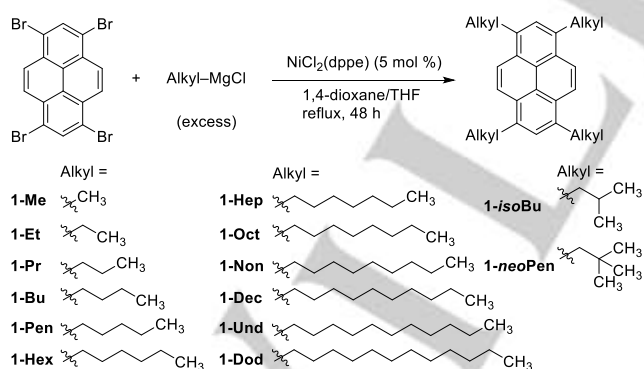
with mono- to tetraalkyl substituents and investigated their photophysical properties, demonstrating the alkyl substituent effects on the pyrene chromophores, but the solid-state photophysical properties were not examined.<sup>[9]</sup> Undoubtedly, the systematic incorporation of alkyl groups is necessary for better utilization of the unique photophysical properties of pyrenes.<sup>[12]</sup>

Herein, we determined the solid-state photophysical properties and molecular orientation of 1,3,6,8-tetraalkylpyrenes bearing linear alkyl or branched alkyl groups. In dilute solutions, 1,3,6,8-tetraalkylpyrenes showed an unchanged luminescence color (Figure 1a) in sharp contrast to that of the crystalline samples of 1,3,6,8-tetraalkylpyrenes depending on the length of the alkyl groups (Figure 1b). The systematic results obtained herein provide a mechanistic understanding of photophysical properties by comparing solution- and solid-state behaviors.

## Results and Discussion

## Synthesis of 1,3,6,8-tetraalkylpyrenes

Twelve pyrenes with four linear alkyl groups at the 1-, 3-, 6-, and 8-positions (Alkyl = Me, Et, Pr, Bu, Pen, Hex, Hep, Oct, Non, Dec, Und, or Dod) were synthesized via Kumada-Tamao-Corriu cross-coupling reaction of 1,3,6,8-tetrabromopyrene with corresponding alkyl Grignard reagents and were obtained in moderate yields (Scheme 1).<sup>[9,12c,13]</sup> The prepared 1,3,6,8-tetraalkylpyrenes were purified by successive silica gel column chromatography, size exclusion chromatography, and recrystallization prior to photophysical analyses. Branched alkyl groups such as isobutyl (**1-isoBu**) and neopentyl (**1-neoPen**) were also introduced to the pyrene ring by following the same procedure. Recrystallization of the 1,3,6,8-tetraalkylpyrenes from  $\text{CHCl}_3/\text{MeOH}$  afforded colorless needle crystals, except for **1-Me**, **1-Et**, and **1-isoBu**, which afforded colorless plate crystals.



Scheme 1. Synthesis of the 1,3,6,8-tetraalkylpyrenes.

## Photophysical properties in solution

The normalized steady-state UV/vis and fluorescence spectra of the prepared 1,3,6,8-tetraalkylpyrenes in  $\text{CH}_2\text{Cl}_2$  ( $1.0 \times 10^{-5}$  M) along with those of the unsubstituted pyrene **2** are shown in Figure 2 (for the UV/vis and fluorescence spectra of each pyrene derivative, see Figures S1–S15), and spectral data are

summarized in Table 1. The introduction of alkyl groups at the 1-, 3-, 6-, and 8-positions of pyrene caused ca.  $2060 \text{ cm}^{-1}$  bathochromic shifts of the overall absorption profile (indicated by the blue lines in Figure 2a) when compared with that of the non-substituted pyrene **2** (orange line in Figure 2a). This bathochromic shift reflects the narrower HOMO-LUMO bandgaps of **1** compared to those of **2**, which were likely caused by increasing the HOMO energy levels via C-H  $\sigma$ - $\pi$  hyper conjugation.<sup>[9,14]</sup> Regardless of the length and branching pattern of the alkyl groups, no significant differences in absorption wavelength and spectral shape among all tetraalkylpyrenes were observed, as shown in the blue trace (Figure 2a). The fluorescence spectra of **1** in  $\text{CH}_2\text{Cl}_2$  also showed a similar tendency (i.e. bathochromic shift when compared with **2**, no significant difference in the series of **1**), with emissions observed at 377, 410, and 430 nm (Figure 2b). The time-resolved fluorescence spectrum of **1-Dod** in a dilute  $\text{CH}_2\text{Cl}_2$  solution indicated that vibronic-structured emissions at 377, 410, and 430 nm correspond to the monomer fluorescence ( $S_1$  to  $S_0$ ), while the long-lived emission at  $>450$  nm is derived from an excimer (Figure S17), which is typical for non-substituted pyrene in solution.<sup>[15]</sup> These observations in the absorption and emission spectra clearly show that the alkyl group structures do not significantly affect the photophysical behavior of the pyrene chromophore in dilute  $\text{CH}_2\text{Cl}_2$  solution.

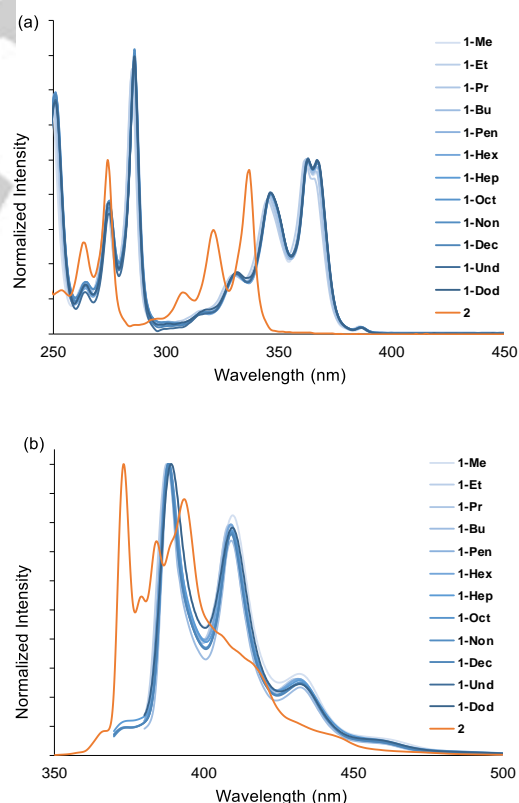


Figure 2. Normalized steady-state absorption (a) and emission (b) spectra of the 1,3,6,8-tetraalkylpyrenes and pyrene in  $\text{CH}_2\text{Cl}_2$  ( $1.0 \times 10^{-5}$  M).

## FULL PAPER

**Table 1.** UV/vis and fluorescence spectral data of the 1,3,6,8-tetraalkylpyrenes and pyrene in the dilute solution<sup>[a]</sup>

	$\lambda_{\max}$ (nm)	$\varepsilon$ ( $10^4$ L mol <sup>-1</sup> cm <sup>-1</sup> ) <sup>[b]</sup>	$\lambda_{\text{em}}$ (nm) <sup>[c]</sup>	Stokes shift $\nu$ (cm <sup>-1</sup> )
<b>2</b>	337	3.7	395, 373	2864
<b>1-Me</b>	363	4.1	431.8, 409.6, 389.0	1841
<b>1-Et</b>	362	4.0	430.8, 408.4, 387.4	1811
<b>1-Pr</b>	362	4.2	431.2, 408.4, 387.8	1838
<b>1-Bu</b>	363	4.0	432.4, 409.2, 388.2	1788
<b>1-Pen</b>	363	4.4	431.6, 408.8, 388.2	1788
<b>1-Hex</b>	363	4.0	431.8, 409.0, 388.2	1788
<b>1-Hep</b>	363	4.4	432.2, 409.4, 388.4	1802
<b>1-Oct</b>	363	4.2	432.2, 409.2, 388.2	1788
<b>1-Non</b>	363	4.4	432.2, 409.4, 388.4	1802
<b>1-Dec</b>	363	4.0	432.2, 409.2, 388.2	1788
<b>1-Und</b>	363	4.2	432.2, 409.2, 388.2	1788
<b>1-Dod</b>	363	4.1	432.2, 409.4, 389.0	1841
<b>1-isoBu</b>	368	4.1	432.4, 409.2, 388.2	1414
<b>1-neoPen</b>	363	4.0	432.4, 409.2, 388.2	1788

[a]  $1.0 \times 10^{-5}$  M in CH<sub>2</sub>Cl<sub>2</sub>. [b] Molar absorptivity coefficient at  $\lambda_{\max}$ . [c]  $\lambda_{\text{ex}} = 320$  nm.

**Table 2.** Steady-state photophysical properties of the 1,3,6,8-tetraalkylpyrenes and pyrene in the solid state<sup>[a]</sup>

	$\lambda_{\max}$ (nm)	$\lambda_{\text{em}}$ (nm) <sup>[a]</sup>	$\Phi_F$
<b>2</b>	–	467	0.68 <sup>[16]</sup>
<b>1-Me</b>	391	445	0.23
<b>1-Et</b>	390	415	0.88
<b>1-Pr</b>	392	433	0.51
<b>1-Bu</b>	373	418	0.79
<b>1-Pen</b>	373	418 <sup>[b]</sup>	0.26
<b>1-Hex</b>	378	419	0.75
<b>1-Hep</b>	370	409	0.79
<b>1-Oct</b>	379	419	0.65
<b>1-Non</b>	379	418	0.44
<b>1-Dec</b>	376	417	0.57
<b>1-Und</b>	378	417	0.63
<b>1-Dod</b>	377	417	0.25
<b>1-isoBu</b>	373	408	0.26
<b>1-neoPen</b>	368	411	0.32

[a]  $\lambda_{\text{ex}} = 320$  nm except for **1-Me** ( $\lambda_{\text{ex}} = 340$  nm). [b] One of the two polymorphism (*vide infra*).

**Photophysical properties in the solid state**

Next, we focused on the solid-state photophysical properties of 1,3,6,8-tetraalkylpyrenes, because they exhibited different luminescence colors in the solid state upon irradiation with UV light (Figure 1b).<sup>[16]</sup> Unsubstituted pyrene **2** showed a light-blue luminescence in the solid state, in sharp contrast to its violet luminescence in the dilute CH<sub>2</sub>Cl<sub>2</sub> solution. On the other hand, the crystalline sample of 1,3,6,8-tetraethylpyrene **1-Et** and many alkylated pyrenes furnished with longer chains showed violet luminescence ( $\lambda_{\text{em}}$  408–419 nm) similar to that observed in solution, indicating the monomer emission is the main decay path of the excited states of the tetraalkylated pyrenes. Pyrenes containing propyl (**1-Pr**) and dodecyl (**1-Dod**) groups showed a similar luminescence color as pyrene due to the mixture of the monomer and excimer emissions.

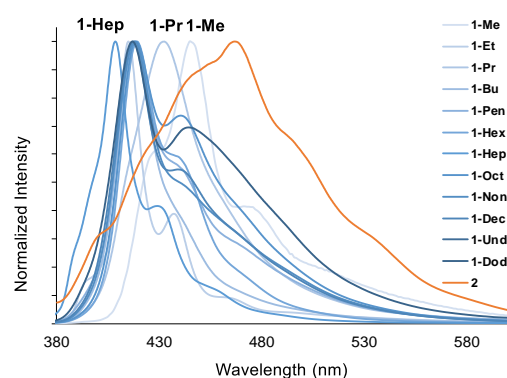
**Figure 3.** Normalized steady-state fluorescence spectra of 1,3,6,8-tetraalkylpyrenes and pyrene **2** in the solid state.

Figure 3 shows the steady-state fluorescence spectra of pyrene **2** and the prepared 1,3,6,8-tetraalkylpyrenes in the solid state. Pyrene **2** exhibited a broad excimer emission peak centered

## FULL PAPER

at 467 nm in the solid state (Figure 3, orange line).<sup>[17]</sup> When Me groups were introduced to the pyrene core, an emission peak was observed at 445 nm along with shoulders at 472 and 430 nm, implying the additional contribution of excimers. Interestingly, **1-Et** showed a sharp emission band at 415 nm, comparable to that observed in the CH<sub>2</sub>Cl<sub>2</sub> solution (408 nm). Although the other 1,3,6,8-tetraalkylpyrenes bearing longer linear alkyl chains, except **1-Pr** and **1-Hep**, showed emission bands at ca. 417–419 nm similar to that of **1-Et**, they were accompanied by broad emission bands at approximately 440 nm. In contrast, **1-Pr** showed  $\lambda_{em}$  at 433 nm and the introduction of heptyl, isobutyl (Figure S14), and neopentyl (Figure S15) groups hypochromically shifted the maxima to 409, 408, and 411 nm, respectively.

Representative time-resolved fluorescence spectra of **1-Et** and **1-Dod** are shown in Figures 4 and 5, respectively. The time-resolved fluorescence spectrum of the solid-state sample of **1-Et** clearly showed that the observed emissions originated from the monomer (Figure 4), suggesting that the pyrene cores are separated in the solid state by Et groups, suppressing excimer formation. In contrast, broad emission bands at approximately 450 nm appeared over several tens of nanoseconds for the **1-Bu** (Figure S18) and **1-Dod** (Figure 5) samples, which were attributed to long-lived excited species compared to the monomer species. The time-resolved fluorescence spectrum of **1-isoBu** ( $\lambda_{em} = 408$  nm) indicated monomer fluorescence rather than that arising from an excimer (Figure S19).

The fluorescence quantum yield ( $\Phi_F$ ) for each compound is listed in Table 2 (For fluorescence lifetime, see: Table S1). It should be noted that, among the prepared 1,3,6,8-tetraalkylpyrenes, pyrenes bearing linear alkyl groups with even-number carbons exhibited high  $\Phi_F$  values except for **1-Dod**. In contrast, pyrenes containing linear alkyl groups with odd-number carbons showed smaller  $\Phi_F$  values for **1-Me**, **1-Pen**, and **1-Non**, and larger  $\Phi_F$  values for **1-Pr**, **1-Hep**, and **1-Und**. This phenomenon may arise from the packing mode of alkyl chains in the solid state, and the more effective interaction of even-numbered alkyl chains between adjacent columns (*vide infra*) suppresses vibrational relaxation to enhance the quantum yields.<sup>[18]</sup> It should be noted that **1-Et** exhibited the highest  $\Phi_F$  of 0.88, higher than that of unsubstituted pyrene **2** ( $\Phi_F = 0.68$ ).<sup>[8,9,17]</sup>

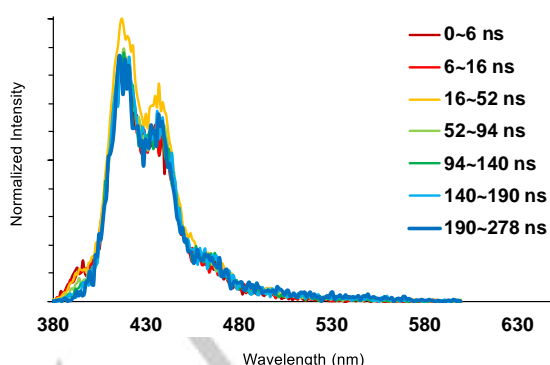


**Figure 4.** Time-resolved fluorescence spectra of **1-Et** in the solid state; brown: 0-6 ns, red: 6-16 ns, orange: 16-52 ns, light green 52-94 ns, green: 94-140 ns, cyan: 140-190 ns, blue: 190-278 ns.

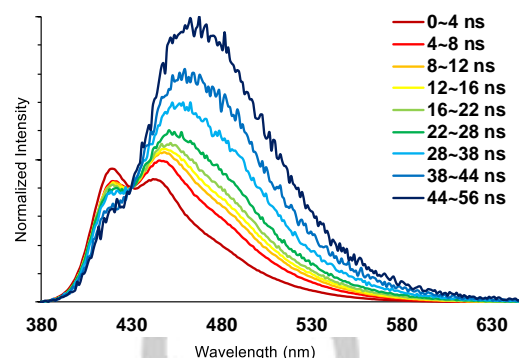


**Figure 5.** Time-resolved fluorescence spectra of **1-Dod** in the solid state; brown: 0-4 ns, red: 4-8 ns, orange: 8-12 ns, yellow: 12-16 ns, light green 16-22 ns, green: 22-28 ns, cyan: 28-38 ns, blue: 38-44 ns, navy blue: 44-56 ns.

We estimated the solid-state fluorescence lifetimes of several pyrene derivatives and found that **1-Et** have two representative lifetimes of ca. 40 and 80 ns (Table S1). In addition, the rate constants for the solid-state fluorescence radiative and nonradiative decays of **1-Bu** were five times and one-fiftieth compared to those in diluted solution, respectively.

These results indicate that the decay pathways, i. e.,  $\Phi_F$ , can be controlled using the alkyl group by varying the molecular orientations in solid state (*vide infra*).

### Crystal structures

To understand the effects of the alkyl chains on the solid-state photophysical properties, X-ray crystallographic analyses were performed. Fine crystals suitable for X-ray crystallography were obtained by recrystallization from CHCl<sub>3</sub> and MeOH for **1-Me**, **1-Et**, **1-Pr**, **1-Bu**, and **1-Pen**. The molecular structures of the 1,3,6,8-tetraalkylpyrenes determined at 123 K are shown in Figure 6.<sup>[19]</sup> It should be noted that the conformation of the alkyl chains was not disordered in all samples and **1-Et** and **1-Pr** adopted similar geometries. The ethyl and propyl groups were oriented orthogonally to the pyrene ring, where two pairs of alkyl group on each side were oriented in the opposite direction ( $C_{2h}$  symmetry).<sup>[20]</sup> In contrast, **1-Bu** and **1-Pen** contained two alkyl groups at the cater-corner positions in the same plane as the pyrene core, and the other two alkyl chains were orthogonal to the pyrene ring and oriented in the opposite direction ( $C_i$  symmetry). The conformation of the alkyl chains was an *anti*-conformation except for the C–C bond between the  $\alpha$ - and  $\beta$ -carbons of the orthogonally oriented Bu and Pen groups (*gauche*-conformation). From theoretical calculations, it was proposed that the Bu groups in the same plane as the pyrene core participated in C–H  $\sigma$ - $\pi$  conjugation (*vide infra*).<sup>[9]</sup>

Although polymorphism was observed for **1-Pen**,  $\lambda_{em}$  and the molecular structure of the pyrene core in the crystals were essentially the same for both forms. In the Figure 6, the molecular structures of the polymorphism are shown, where two asymmetric units of the isolated pair reside in the crystal. Differences in the asymmetric units manifested in the orientation of the terminal methyl groups of the pentyl groups that were in the same plane as the pyrene ring and the terminal propyl groups of the

## FULL PAPER

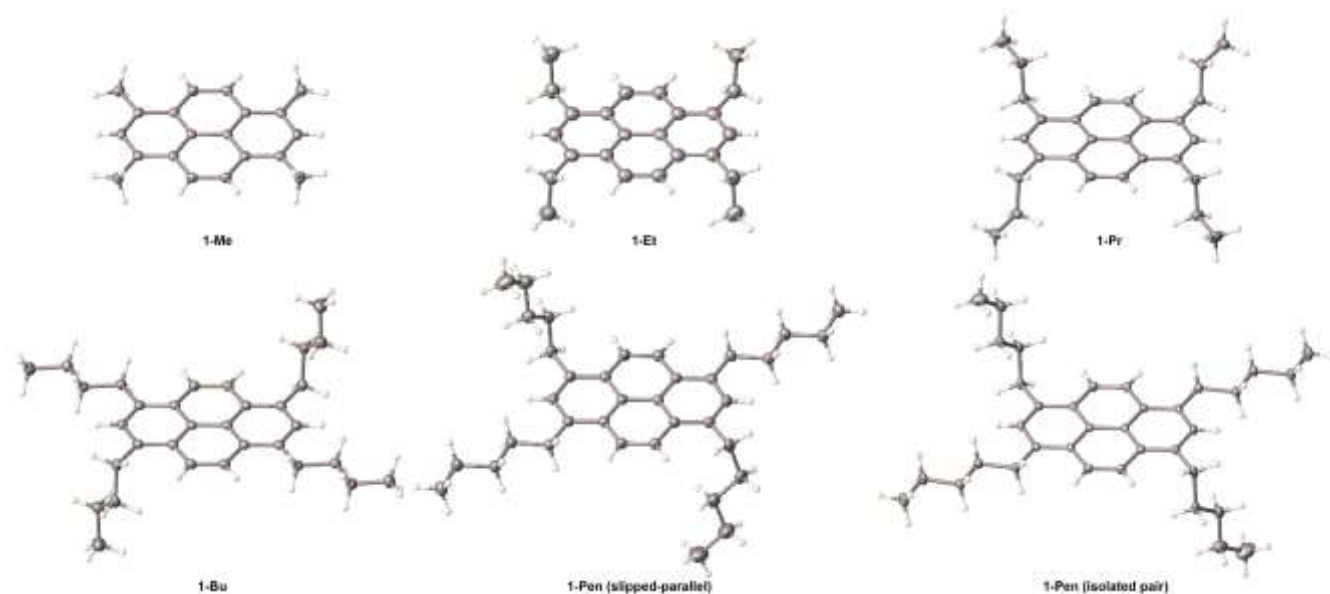


**Figure 6.** Molecular structures of the 1,3,6,8-tetraalkylpyrenes bearing linear alkyl groups in the crystal.

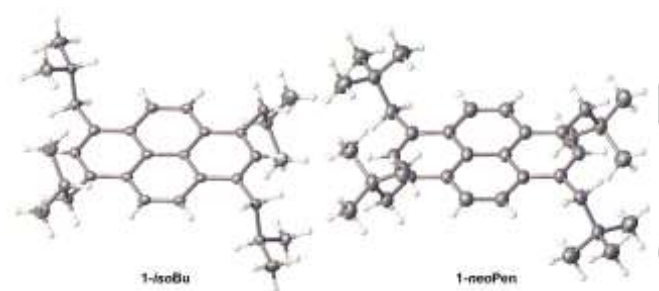


**Figure 7.** Molecular structures of the 1,3,6,8-tetraalkylpyrenes bearing branched alkyl groups in the crystal.

orthogonally oriented pentyl groups. All pentyl groups of one of the asymmetric units adopted an *anti*-conformation, whereas the two pentyl groups in the same plane as the pyrene ring in the other asymmetric unit adopted a *gauche*-conformation for the terminal methyl group. The polymorphism likely arose from conformational differences of the alkyl chains, which affected the interaction between adjacent columns (*vide infra*).

The branched alkyl groups in **1-isoBu** and **1-neoPen** adopted the same orientations, in which the two pairs of alkyl groups occupied the orthogonal position on opposite sides of the pyrene ring ( $C_{2h}$  symmetry; Figure 7).

### Crystal packing

Herein, we obtained three types of packing systems, which were categorized as herringbone (**1-Me**, **1-Et**, and **1-isoBu**), slipped-parallel (**1-Pr**, **1-Bu**, **1-Pen**, and **1-neoPen**), or isolated-pair types (**1-Pen**).<sup>[21]</sup> For **1-Pen**, polymorphism, including slipped-parallel and isolated-pair types, was observed (*vide supra*).

#### Herringbone packing

For **1-Me**, **1-Et**, and **1-isoBu**, the molecular orientation in the crystal was classified as herringbone, and the vertical distances ( $v$ ) between the two parallel pyrene cores were 3.524, 4.982, and 7.153 Å, respectively.<sup>[25]</sup> The face-to-face pair of **1-Me** and **1-Et** slipped toward the short axis ( $s$ ) of pyrene by 4.316 and 5.320 Å, respectively, whereas that of **1-isoBu** slipped towards the long axis ( $l$ ) of pyrene by 5.342 Å. As the distance of the two parallel

**Table 3.** Distances between the two pyrene cores.

	$v$ (Å)	$l$ (Å)	$s$ (Å)	$c$ (Å)
<b>1-Me</b>	3.543	0.022	4.316	6.276
<b>1-Et</b>	4.982	0.086	5.320	6.283
<b>1-isoBu</b>	7.153	5.342	0.534	7.109
<b>2 (Form I)</b> <sup>[22]</sup>	5.929	4.584	4.966	7.207
<b>2 (Form II)</b> <sup>[23]</sup>	5.764	6.692	7.792	6.611
<b>2 (Form III)</b> <sup>[24]</sup>	3.472	1.668	0.084	7.913

## FULL PAPER

pyrene cores ( $\nu$ ) decreased, the emission wavelength exhibited a bathochromic shift (**1-Me** = 445 nm, **1-Et** = 415 nm, and **1-isoBu** = 408 nm). The theoretical calculations suggested that pyrene formed an excimer with distances between the two parallel pyrene rings of 3.410 Å for  $\nu$  and 1.524 Å for  $l$ .<sup>[26]</sup> These calculations support the model where **1-Me** forms an excimer in the crystal, resulting in an emission band at 445 nm. In contrast, for **1-Et** and **1-isoBu**, pyrene chromophores were separated by alkyl groups, suppressing excimer formation. These molecular orientations in the crystals are consistent with the observed emission spectra (**1-Me** = 445 nm, **1-Et** = 415 nm, and **1-isoBu** = 408 nm).

It is well-known that pyrene **2** also forms herringbone-type packing, and three polymorphic forms were reported, as summarized in Table 3. In forms I and II, the distance between the two pyrene cores in the face-to-face orientation is  $>5.7$  Å, indicating that the two pyrene cores shift toward both the long and short axes, resulting in a large void between them. Therefore, an exciton could couple with an adjacent pyrene even in the solid state, resulting in a broad excimer emission at approximately 467 nm. However, for **1-Et** and **1-isoBu**, orthogonally oriented alkyl groups filled the void between the two parallel pyrene rings, suppressing excimer formation.

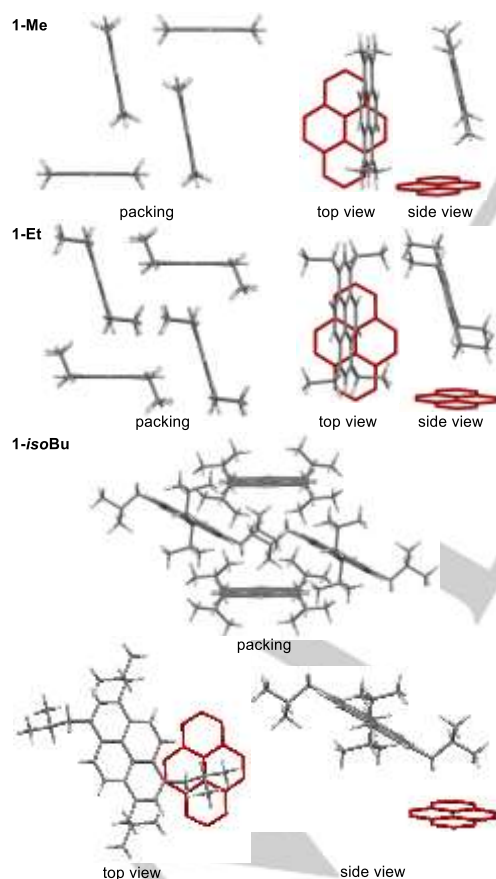


**Figure 8.** Packing mode and interactions between the orthogonally oriented pyrene cores in herringbone-type packing. Alkyl groups on one of the two 1,3,6,8-tetraalkylpyrenes were omitted for clarity.

Among the 1,3,6,8-tetraalkylpyrenes examined, **1-Et** with herringbone-type packing showed the highest quantum yield ( $\Phi_F$ ) of 0.88, higher than that of the parent pyrene **2** as well as **1-Me** and **1-isoBu**, which have shorter and longer  $\nu$  values, respectively. This is likely due to the short contacts between the orthogonally oriented pyrenes via aromatic and aliphatic C-H $\pi$  interactions that immobilize excitons (Figure 8). Indeed, the Et groups infilled the space between the pyrene cores and formed multiple C-H $\pi$  interactions, preventing excimer formation and facilitating non-emitting vibrational relaxation. Although the orientation of the two orthogonally oriented pyrene cores in **1-Me** was quite similar to that of **1-Et** (Figure 8, top and middle), its  $\Phi_F$  was significantly lower compared to that of **1-Et**.

In contrast, the contact between the orthogonally oriented pyrene cores of **1-isoBu** occurs via a four-point C-H $\pi$  interaction between the benzylic methylene and one methyl group (Figure 8, bottom). This suggests that the predominant C-H $\pi$  interaction of the sterically hindered alkyl group occurs in aliphatic C-H bonds rather than in aromatic C-H bonds.

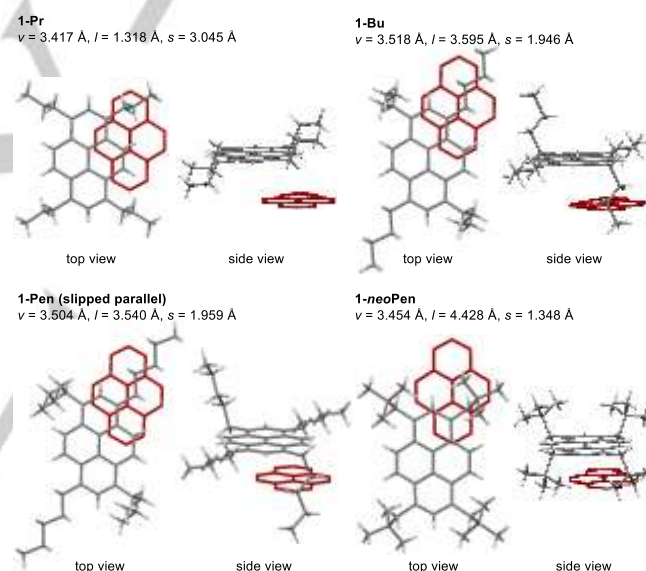


**Figure 9.** Interactions between the orthogonally oriented pyrene cores in slipped-parallel-type packing.

#### Slipped-parallel

The solid-state photophysical properties of 1,3,6,8-tetraalkylpyrenes exhibiting slipped-parallel-type packing structure can be discussed with respect to the relative position of the two parallel pyrene rings. Figure 9 shows the two pyrene rings of **1-Pr**, **1-Bu**, **1-Pen** (slipped-parallel), and **1-neoPen**, where alkyl groups on one of the two 1,3,6,8-tetraalkylpyrenes were omitted for clarity, and face-to-face distances ( $\nu$ ) and slipped distances between the centers of the pyrene rings in the long ( $l$ ) and short ( $s$ ) axes are shown. It should be noted that the face-to-face distance between the two pyrene rings ( $\nu$ ) was similar for all samples (3.417–3.518 Å). In contrast, a significant difference was

## FULL PAPER

observed in slipping of the two pyrene cores (*s* and *l*), where **1-Pr** largely shifted toward the short axis (*s*) by 3.045 Å rather than the long axis (*l* = 1.318 Å). These parameters (*s* and *l*) of **1-Bu** were 1.946 and 3.595 Å, respectively, and **1-Pen** and **1-neoPen** showed a similar slipping mode as that of **1-Bu**. In these cases, the two methylenes at the  $\alpha$ - and  $\beta$ -positions of one alkyl group contributed to the C-H- $\pi$  interaction, which is in sharp contrast with **1-Pr**, where two C-H bonds of the  $\alpha$ -methylene formed a C-H- $\pi$  interaction. The **1-Pr** compound showed a significant bathochromic shift ( $\lambda_{em}$  = 433 nm) in its solid-state fluorescence spectrum, where the slipping distance along the long axis (*l*) was short (1.318 Å). For **1-Bu** and **1-Pen**, the two pyrene rings slipped by 3.595 and 3.540 Å, respectively, along the long axis, and  $\lambda_{em}$  was observed at 418 nm. Slipping in the long axis direction increased (*l* = 4.428 Å) when *neoPen* was introduced, and the fluorescence spectrum was not largely changed compared to spectrum of the compound in the dilute solution. These results indicate that the slipping toward the long axis rather than the short axis significantly contributed to the suppression of excimer formation in the solid state.

Among the four abovementioned pyrene derivatives, **1-Bu** showed the best quantum yield ( $\Phi_F$ ) of 0.79. The formation of C-H- $\pi$  interactions between the pyrene core and Bu group in-plane likely contributed to the suppression of vibrational relaxation.<sup>[27]</sup>

#### Isolated-pair

The polymorphism was observed in the X-ray crystallographic analysis of **1-Pen**, involving slipped-parallel and isolated-pair-type packings. Both packing modes contained independent columns (Figure 10), including a slipped-parallel stacking in the same manner as that of **1-Bu**. Therefore, the face-to-face interaction between pyrene cores was essentially unchanged, and the distances between the two pyrene cores in the face-to-face orientation ranged from  $v$  = 3.499 to 3.604, *l* = 3.412 to 3.561, and *s* = 1.983 to 1.959 Å.

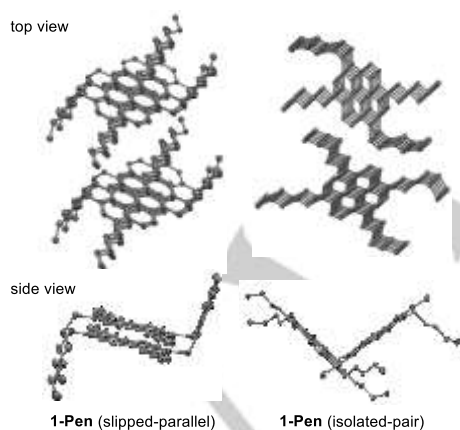


**Figure 10.** Two polymorphism of **1-Pen** and its packings. H atoms were omitted for clarity

The difference in the packing of the two polymorphic forms is the orientation of columns, where columns are directed in a parallel and staggered manner in the slipped-parallel and

isolated-pair-type crystals, respectively (Figure 10, side view). These differences in the relative orientation of adjacent columns likely arise from the weak van der Waals interactions between the alkyl groups.

The polymorphic samples of **1-Pen** showed a slightly different solid-state emission. The crystals of slipped-parallel and isolated-pair **1-Pen** exhibited  $\lambda_{em}$  at 421 and 418 nm, respectively. The slipped-parallel crystals also showed relatively high intensities at ca. 440 and 470 nm than isolated-pair crystals. The drop-casted sample of **1-Pen** showed a broad emission at 471 nm, which is in sharp contrast to the same fluorescence profile of **1-Et** in crystal and film forms (Figures S22 and S23).

## Conclusions

We demonstrated the systematic synthesis of 1,3,6,8-tetraalkylpyrenes with 14 different alkyl groups and the subsequent determination of their solid-state photophysical properties. The introduction of alkyl groups at the 1-, 3-, 6-, and 8-positions caused bathochromic shifts in the emission wavelength from the parent pyrene, but emission peaks did not vary based on the structures of the alkyl groups in the dilute solution. However, in the solid state, emission wavelengths and quantum yields varied depending on the structures of the introduced alkyl chains. Among the pyrene derivatives examined, tetraethylpyrene **1-Et** showed the highest fluorescence quantum yield of 0.88, higher than the parent pyrene. The fluorescence maximum of **1-Et** in the solid state did not shift from that observed in solution, in contrast to the large bathochromic shift (5396  $\text{cm}^{-1}$ ) of pyrene in the solid state, which is a result of excimer formation.

The molecular orientation of the 1,3,6,8-tetraalkylpyrenes in crystal form was revealed by X-ray crystallography and categorized into three types, namely herringbone, slipped-parallel, or isolated-pair-type. Comparison of the relative orientation of pyrene cores in the crystals indicated that the face-to-face and slipping distances along the long axis of the pyrene ring exerted strong effects on photophysical properties likely due to excimer formation. The alkyl groups affected the emission color and quantum yield. Interactions between the pyrene core and alkyl groups through C-H- $\pi$  interaction improved the fluorescence quantum yield by suppressing the vibrational relaxation of excitons.

Although alkyl groups are often introduced to functional materials and/or  $\pi$ -molecules to improve their solubility and stability, the effects of these groups on the properties of the materials have not been systematically examined in many cases. It was demonstrated that the alkyl groups exerted no significant electronic effects on the chromophores, but largely contributed to the emission color and quantum yields in the solid state by modifying the molecular orientation of the crystals. Both the length and branching of the alkyl substituents were important for controlling the solid-state photophysical properties, which may be expandable to other chromophoric materials and  $\pi$ -systems.

## Experimental Section

## FULL PAPER

**General:** All reactions using air- and moisture-sensitive compounds were carried out by the standard Schlenk techniques under a nitrogen atmosphere unless otherwise noted. Dehydrated THF were purchased from Kanto Chemical Company and purified by SPS<sup>[28]</sup> prior to use. Dehydrated 1,4-dioxane was purchased from Wako Pure Chemical Industries and used as received. Grignard reagents were prepared by a standard procedure or purchased from Aldrich or TCI. These Grignard reagents were used after titration using I<sub>2</sub>. 1,3,6,8-Tetrabromopyrene was prepared according to literature.<sup>[29]</sup> Analytical grade CH<sub>2</sub>Cl<sub>2</sub> for UV-Vis and fluorescence measurements was purchased from Kishida and was used as received.

**Synthesis of 1,3,6,8-tetraalkylpyrenes:**<sup>[12c]</sup> To a 100 mL three necked flask containing 1,3,6,8-tetrabromopyrene (414 mg, 0.80 mmol) and NiCl<sub>2</sub>(dppe) (21 mg, 0.04 mmol) was added 1,4-dioxane (24 mL) and RMgCl (in THF, 9.6 mmol). After refluxing for 48 h, 1 M HCl aq. was carefully added to the reaction mixture and then diluted by 50 mL of H<sub>2</sub>O. The aqueous layer was extracted by Et<sub>2</sub>O (50 mL x 2). The organic layer was dried over Na<sub>2</sub>SO<sub>4</sub>, concentrated, and purified by silica gel column chromatography (eluent: hexane or hexane/EtOAc = 9/1). Further purification by GPC (eluent: CHCl<sub>3</sub>) followed by recrystallization from CH<sub>3</sub>Cl/MeOH (twice) gave a pure sample for the analysis of photophysical properties.

**Steady-state UV/Vis absorption and fluorescence spectroscopy:** UV/Vis and fluorescence measurements in solution were performed with a U-3500 UV/Vis spectrophotometer (HITACHI) and a FP-8500 spectrofluorometer (Jasco), respectively. The samples were dissolved in CH<sub>2</sub>Cl<sub>2</sub> (1.0 x 10<sup>-5</sup> M).

**Solid-state UV/Vis absorption and fluorescence spectroscopy and quantum yields:** UV/Vis measurements of crystalline samples were performed with a V-770 UV/Vis spectrophotometer (Jasco). Fluorescence and fluorescence quantum yields of crystalline samples were measured on a FP-6500 spectrofluorometer (Jasco) with ISF-513 fluorescence integrate sphere unit (Jasco).

**Time-resolved fluorescence spectroscopy:** Time-resolved spectroscopic measurement was conducted with a time-correlated single-photon counting fluorometer (Quantaaurus-Tau C11367, Hamamatsu Photonics).

**Crystal structure determinations:** X-ray crystallographic measurements were made on a Rigaku RAXIS-RAPID diffractometer with a 2-D area detector using graphite-monochromated Cu-K $\alpha$  radiation ( $\lambda = 1.54187 \text{ \AA}$ ) or a Rigaku XtaLAB Synergy diffractometer with a HyPix detector using mirror-monochromated Cu-K $\alpha$  ( $\lambda = 1.54184 \text{ \AA}$ ) or Mo-K $\alpha$  ( $\lambda = 0.71073 \text{ \AA}$ ) radiation. Crystals were mounted on a glass fiber and placed in a nitrogen stream at 123(2) K. The structures were solved by direct methods (SHELXS97,<sup>[30]</sup> SHELXT,<sup>[31]</sup> or SIR2008<sup>[32]</sup>). The structure was refined on  $F^2$  by the full-matrix least-squares method using SHELXL97<sup>[30]</sup> or OLEX2<sup>[33]</sup>. The non-hydrogen atoms were anisotropically refined, while the hydrogen atoms were refined using the riding model.

CCDC 1939308 (1-Me at 123 K), 1939309 (1-Et at 123 K), 1939310 (1-Pr at 123 K), 1939311 (1-Bu at 123 K), 1939312 (1-Pen (Slipped-parallel) at 123 K), 1939313 (1-Pen (Isolated-pair) at 123 K), 1939314 (1-isoBu at 123 K), 1939315 (1-neoPen at 123 K), 1939316 (1-Et at 293 K), 1939317 (1-Pr at 293 K), and 1939318 (1-isoBu at 293 K) contain the supplementary crystallographic data for this paper. These data are provided free of charge by The Cambridge Crystallographic Data Center.

## Acknowledgements

This work was partially supported by a Grant-in-Aid for Scientific Research (A) (JP25248025, to NK), a Grant-in-Aid for Young Scientists (A) (JP16H06039, to TI), and Grant-in-Aid for Scientific Research on Innovative Areas "Middle Molecular Strategy" (JP16H01150 and JP18H04410, to TI) and " $\pi$ -System Figuration" (JP17H05155, to YT). The computations were performed using the Research Center for Computational Science, Okazaki, Japan.

**Keywords:** alkyl • crystal engineering • fluorescence • pyrene • solid-state structure

- [1] For a review, see: T. M. Figueira-Duarte, K. Müllen, *Chem. Rev.* **2011**, *111*, 7260.
- [2] a) T. Oyamada, S. Akiyama, M. Yahiro, M. Saigou, M. Shiro, H. Sasabe, C. Adachi, *Chem. Phys. Lett.* **2006**, *421*, 295; b) S. Bernhardt, M. Kastler, V. Enkelmann, M. Baumgarten, K. Müllen, *Chem. Eur. J.* **2006**, *12*, 6117; c) Y. Sagara, T. Mutai, I. Yoshikawa, K. Araki, *J. Am. Chem. Soc.* **2007**, *129*, 1520; d) J. N. Moorthy, P. Natarajan, P. Venkatakrisnan, D.-F. Huang, T. J. Chow, *Org. Lett.* **2007**, *9*, 5215; e) P. Anant, N. T. Lucas, J. M. Ball, T. D. Anthopoulos, J. Jacob, *Synth. Metals* **2010**, *160*, 1987; f) G. Wang, J. Geng, X. Zhang, L. Cai, D. Ding, K. Li, L. Wang, Y.-H. Lai, B. Liu, *Polym. Chem.* **2012**, *3*, 2464; g) R. R. Reghu, J. V. Grazulevicius, J. Simokaitiene, A. Miasojedovas, K. Kazlauskas, S. Jursenas, P. Data, K. Karon, M. Lapkowski, V. Gaidelis, V. Jankauskas, *J. Phys. Chem. C* **2012**, *116*, 15878; h) S. Yamaguchi, I. Yoshikawa, T. Mutai, K. Araki, *J. Mater. Chem.* **2012**, *22*, 20065; i) J.-Y. Hu, X. Feng, H. Tomiyasu, N. Seto, U. Rayhan, M. R. J. Elsegood, C. Redshaw, T. Yamato, *J. Mol. Struct.* **2013**, *1047*, 194; j) K. R. Idzik, T. Licha, V. Lukeš, P. Rapta, J. Frydel, M. Schaffer, E. Tauscher, R. Beckert, L. Dunsch, *J. Fluoresc.* **2014**, *24*, 153; k) M. Sang, S. Cao, J. Yi, J. Huang, W.-Y. Lai, W. Huang, *RSC Adv.* **2016**, *6*, 6266; l) T. H. El-Assaad, M. Auer, R. Castañeda, K. M. Hallal, F. M. Jradi, L. Mosca, R. S. Khnayzer, D. Patra, T. V. Timofeeva, J.-L. Brédas, E. J. W. List-Kratochvil, B. Wex, B. R. Kaafarani, *J. Mater. Chem. C* **2016**, *4*, 3041; m) R. K. Konidena, K. R. J. Thomas, M. Singh, J.-H. Jou, *J. Mater. Chem. C* **2016**, *4*, 4246; n) K. P. Gan, M. Yoshio, T. Kato, *J. Mater. Chem. C* **2016**, *4*, 5073.
- [3] J. A. Mikroyannidis, *Synth. Mat.* **2005**, *155*, 125.
- [4] a) H. Maeda, T. Maeda, K. Mizuno, K. Fujimoto, H. Shimizu, M. Inouye, *Chem. Eur. J.* **2006**, *12*, 824; b) K. Fujimoto, H. Shimizu, M. Furusyo, S. Akiyama, M. Ishida, U. Furukawa, T. Yokoo, M. Inouye, *Tetrahedron* **2009**, *65*, 9357; c) H. M. Kim, Y. O. Lee, C. S. Lim, J. S. Kim, B. R. Cho, *J. Org. Chem.* **2008**, *73*, 5127; d) G. Venkataramana, S. Sankararaman, *Eur. J. Org. Chem.* **2005**, 4162; e) A. Hayer, V. de Halleux, A. Köhler, A. El-Garouhy, E. W. Meijer, J. Barberá, J. Tant, J. Levin, M. Lehmann, J. Gierschner, J. Cornil, Y. H. Geerts, *J. Phys. Chem. B* **2006**, *110*, 7653; f) K. R. J. Thomas, N. Kapoor, M. N. K. P. Bolisetty, J.-H. Jou, Y.-L. Chen, Y.-C. Jou, *J. Org. Chem.* **2012**, *77*, 3921; g) F. Xu, T. Nishida, K. Shinohara, L. Peng, M. Takezaki, T. Kamada, H. Akashi, H. Nakamura, K. Sugiyama, K. Ohta, A. Orita, J. Otera, *Organometallics* **2017**, *36*, 556; h) C. L. Devi, K. Yesudas, N. S. Makarov, V. J. Rao, K. Bhanuprakash, J. W. Perry, *J. Mater. Chem. C* **2015**, *3*, 3730; i) X. Feng, H. Tomiyasu, J.-Y. Hu, X. Wei, C. Redshaw, M. R. J. Elsegood, L. Horsburgh, S. J. Teat, T. Yamato, *J. Org. Chem.* **2015**, *80*, 10973; j) S. Diring, F. Camerel, B. Donnio, T. Dintzer, S. Toffanin, R. Capelli, M. Muccini, R. Ziessel, *J. Am. Chem. Soc.* **2009**, *131*, 18177; k) P. E. Gama, R. J. Corrêa, S. J. Garden, *J. Lumin.* **2015**, *161*, 37.
- [5] R. Muangpaisal, M.-C. Ho, T.-H. Huang, C.-H. Chen, J.-Y. Shen, J.-S. Ni, J.-T. Lin, T.-H. Ke, L.-Y. Chen, C.-C. Wu, C. Tsai, *Org. Elect.* **2014**, *15*, 2148.
- [6] F. M. Winnik, *Chem. Rev.* **1993**, *93*, 587.

## FULL PAPER

- [7] S. Xue, X. Qiu, Q. Sun, W. Yang, *J. Mater. Chem. C* **2016**, *4*, 1568.
- [8] It is known that alkyl substitution(s) improves fluorescence quantum yield due to the stabilization of S<sub>1</sub> state rather than triplet states by C-H  $\sigma$ - $\pi$  and/or C-C  $\sigma$ - $\pi$  hyperconjugation to suppress intersystem crossing, see: N. Nijegorodov, V. Vasilenko, P. Monowe, M. Masale, *Spectrochim. Acta A* **2009**, *74*, 188.
- [9] Y. Niko, S. Kawauchi, S. Otsu, K. Tokumaru, G.-i. Konishi, *J. Org. Chem.* **2013**, *78*, 3196.
- [10] C. Kitamura, Y. Abe, T. Ohara, A. Yoneda, T. Kawase, T. Kobayashi, H. Naito, T. Komatsu, *Chem. Eur. J.* **2010**, *16*, 890.
- [11] For phenyleneethynylene: a) R. Thomas, S. Varghese, G. U. Kulkarni, *J. Mater. Chem.* **2009**, *19*, 4401; For diphenylbutadiene: b) R. Davis, N. P. Rath, S. Das, *Chem. Commun.* **2004**, *74*; c) R. Davis, N. S. S. Kumar, S. Abraham, C. H. Suresh, N. P. Rath, N. Tamaoki, S. Das, *J. Phys. Chem. C* **2008**, *112*, 2137; For BN-substituted tetrathienonaphthalene: d) X.-Y. Wang, F.-D. Zhuang, X. Zhou, D.-C. Yang, J.-Y. Wang, J. Pei, *J. Mater. Chem. C* **2014**, *2*, 8152; For styrylanthracene: e) W. Liu, Y. Wang, L. Bu, J. Li, M. Sun, D. Zhang, M. Zheng, C. Yang, S. Xue, W. Yang, *J. Lumin.* **2013**, *143*, 50; f) M. Zheng, D. T. Zhang, M. X. Sun, Y. P. Li, T. L. Liu, S. F. Xue, W. J. Yang, *J. Mater. Chem. C* **2014**, *2*, 1913; g) F. Li, N. Gao, H. Xu, W. Liu, H. Shang, W. Yang, M. Zhang, *Chem. Eur. J.* **2014**, *20*, 9991.
- [12] 1,3,6,8-Tetraalkylpyrenes have sporadically reported, see: a) M. Banerjee, V. S. Vyas, S. V. Lindeman, R. Rathore, *Chem. Commun.* **2008**, 1889; b) J. Li, S. Takahashi, N. Fujinuma, K. Endo, M. Yamashita, H. Matsuzaki, H. Okamoto, K. Sawabe, T. Takenobu, Y. Iwasa, *J. Mater. Chem.* **2011**, *21*, 17662; c) C. Diner, D. E. Scott, R. R. Tykwinski, M. R. Gray, J. R. Stryker, *J. Org. Chem.* **2015**, *80*, 1719.
- [13] In order to introduce alkyl group(s) into  $\pi$ -conjugated systems, Sonogashira coupling reaction and subsequent reduction of alkyne are often employed. For instance, see: N. Kulisic, S. More, A. Mateo-Alonso, *Chem. Commun.* **2011**, *47*, 514.
- [14] DFT calculation of **1-Et** and **2** revealed that the orbitals of LUMO and HOMO are essentially the same (Figure S16).
- [15] K. Yoshihara, T. Kasuya, A. Inoue, S. Nagakura, *Chem. Phys. Lett.* **1971**, *9*, 469.
- [16] a) M. Shimizu, T. Hiyama, *Chem. Asian J.* **2010**, *5*, 1516; b) S. Varghese, S. Das, *J. Phys. Chem. Lett.* **2011**, *2*, 863; c) J. Gierschner, S. Y. Park, *J. Mater. Chem. C* **2013**, *1*, 5818; d) F. Würthner, C. R. Saha-Möller, B. Fimmel, S. Ogi, P. Leowanawat, D. Schmidt, *Chem. Rev.* **2016**, *116*, 962; e) J. Gierschner, S. Varghese, S. Y. Park, *Adv. Optical. Mater.* **2016**, *4*, 348.
- [17] R. Katoh, K. Suzuki, A. Furube, M. Kotani, K. Tokumaru, *J. Phys. Chem. C* **2009**, *113*, 2961.
- [18] It is reported that compounds having even-numbered alkyl groups exhibited higher melting points than that having odd-numbered ones, see: a) A. Watanabe, *Bull. Chem. Soc. Jpn.* **1963**, *36*, 336; b) A. A. Schaerer, C. J. Busso, A. E. Smith, L. B. Skinner, *J. Am. Chem. Soc.* **1955**, *77*, 2017.
- [19] We also conducted X-ray analysis at 293 K and obtained essentially the same results. For crystal structure of **1-Et**, cell parameters elongated ca. 1% for each direction at 293 K. See SI.
- [20] DFT calculation of **1-Et** revealed that the energy difference between rotamers arising from the relative orientation of four ethyl groups was within 2 kJ/mol. Among the rotamers, all *syn* orientation was the most energetically stable, and the X-ray structure (3,6-*anti*) had 1.28 kJ/mol higher energy (Figure S21).
- [21] M. Mas-Torrent, C. Rovira, *Chem. Rev.* **2011**, *111*, 4833.
- [22] Y. Kai, F. Hama, N. Yasuoka, N. Kasai, *Acta Cryst. B* **1978**, *34*, 1263.
- [23] C. S. Frampton, K. S. Knight, N. Shankland, K. Shankland, *J. Mol. Struct.* **2000**, *520*, 29.
- [24] F. P. A. Fabbiani, D. R. Allan, S. Parsons, C. R. Pulham, *Acta Cryst. B* **2006**, *62*, 826.
- [25] A similar packing was reported for 1,3,6,8-tetraisopropylpyrene though solid-state photophysical properties have not been documented. See ref 12a.
- [26] N. J. Silva, F. B. C. Machado, H. Lischka, A. J. A. Aquino, *Phys. Chem. Chem. Phys.* **2016**, *18*, 22300. The slipping distance for short axis (*s*) is calculated to be 0 due to the C<sub>2h</sub> symmetry.
- [27] 1,3,6,8-Tetraoct-1-yn-1-ylpyrene also showed a similar packing, where three methylene C-H bonds at 3-, 4-, and 5-positions in octynyl group formed C-H- $\pi$  interaction. See Ref 13.
- [28] A. M. Pangborn, M. A. Giardello, R. H. Grubbs, R. K. Rosen, F. J. Timmers, *Organometallics* **1996**, *15*, 1518.
- [29] H. Vollmann, H. Becker, M. Corell, H. Streeck, *Justus Liebigs Ann. Chem.* **1937**, *531*, 1.
- [30] G. M. Sheldrick, *Acta Cryst. A* **2008**, *64*, 112.
- [31] G. M. Sheldrick, *Acta Cryst. A* **2015**, *71*, 3.
- [32] M. C. Burla, R. Caliandro, M. Camalli, B. Carrozzini, G. L. Casciarano, L. De Caro, C. Giacovazzo, G. Polidori, D. Siliqi, R. Spagna, *J. Appl. Cryst.* **2007**, *40*, 609.
- [33] L. J. Bourhis, O. V. Dolomanov, R. J. Gildea, J. A. K. Howard, H. Puschmann, *Acta Cryst. A* **2015**, *71*, 59.

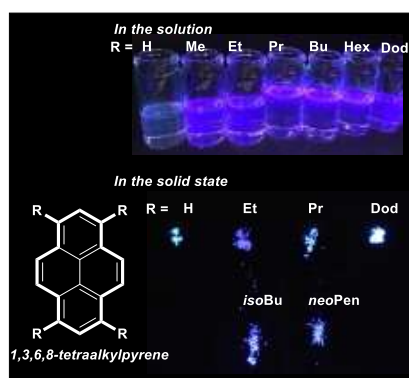
## FULL PAPER

## Entry for the Table of Contents (Please choose one layout)

Layout 1:

## FULL PAPER

This study details systematical evaluation of the fluorescent properties of 1,3,6,8-tetraalkylpyrenes with various alkyl substituents in both the solution and solid states. Although bathochromic shifts were observed for unsubstituted pyrene in the emission spectrum of the solid-state from those of solution state, tetraalkylpyrenes bearing appropriate alkyl groups showed violet luminescence in the solid state similar to that observed in dilute solutions.



T. Iwasaki,\* S. Murakami, Y. Takeda, G. Fukuhara, N. Tohnai, Y. Yakiyama, H. Sakurai, N. Kambe\*

Page No. – Page No.

**Molecular Packing and Solid-state Photophysical Properties of 1,3,6,8-Tetraalkylpyrenes**